

# Modeling and Numerical Simulation of Multi-Destination Pedestrian Crowds

Günter Bärwolff, Tobias Ahnert, Minjie Chen, Frank Huth, Matthias Plaue,  
Hartmut Schwandt

Technische Universität Berlin, Institut für Mathematik  
Straße des 17. Juni 136, 10623 Berlin, Germany  
{baerwolff,ahnert,chenmin,huth,plaue,schwandt}@math.tu-berlin.de  
<http://www.math.tu-berlin.de/projekte/smdpc>

**Abstract.** In this paper we collect two parts of a research project on the pedestrian flow modeling. Rapid growth in the volume of public transport and the need for its reasonable, efficient planning has made the description and modeling of transport and pedestrian behaviors an important research topic in the last twenty years. Comparatively little attention has been paid to the problem of pedestrian crowd behaviors in geometries with multiple destinations: each of the possibly many pedestrians moves to one out of a number of destinations. The objective of the present study is to investigate pedestrian behaviors in such a context. The central problem is the modeling of crossing pedestrian streams. In view of a desirable practical relevance, realistic, i.e. rather complex geometries are studied in this context.

**Keywords:** macroscopic models, pedestrian density and flow measurement, human crowd experiments, intersecting pedestrian flows

## 1 Introduction

In a close cooperation with engineers we investigate the mathematical description of pedestrian movement by

1. data generation with real world experiments for model validation and parameter calibration,
2. development of
  - (a) microscopic mathematical models,
  - (b) macroscopic mathematical models.

We managed the experiments with about 300 students of the TU Berlin and recorded the different constellations of pedestrian streams by a multi-trace recorder as a base for generation of individual tracks and a density estimation.

As microscopic models we discuss grid-based approaches rooted in cellular automata and a second ansatz with a combination of a force-based and a graph-based approach. The microscopic models are discussed in detail for example in [?] and [?].

In this paper we are focused on macroscopic models based on a set of pedestrian-specific coupled partial differential equations (pde's). The first discussed model is based on the mass balance and the considered quantities are the pedestrian density and fluxes which give information about the velocities of pedestrian groups.

As a second model we consider multispecies pedestrian model based on a 3d multiphase incompressible fluid flow model

## 2 A compressible macroscopic model

This macroscopic approach is based on a set of pedestrian-specific coupled partial differential equations. The equations are not derived from the Euler-/Navier-Stokes equations known from fluid and gas dynamics. The specific situation of multi-destination pedestrian crowds with crossing streams requires the development of appropriately adapted methods. This has been targeted by the use of simple heuristics.

Typical applications of these approaches include real-world scenarios like airports, shopping malls, buildings of middle- to large size etc., where the participants (i.e. the pedestrians) do not exhibit an overall unanimity and (may) have different and multiple destinations.

Beyond the modeling of the above-mentioned problems, a particular aim of this project will be the development, implementation and test of appropriate computer-based simulation models.

### 2.1 The Transport Equation

Perceiving pedestrian flows as a transport problem, we start with the governing equation that describes the mass flow:

$$\frac{\partial \rho_i}{\partial \vartheta} + \nabla \cdot (\rho_i v_i) = 0. \quad (1)$$

In this document,  $\vartheta$  denotes the time, and  $i \in \{1, \dots, n\}$  where  $n$  is the number of pedestrian “types” or “species” distinguished by certain properties. The desired velocity would be a frequent example of such a property. Furthermore,  $\rho_i$  is the current density and  $v_i$  the current velocity of a species in a given computational domain.

Since pedestrian dynamics cannot be entirely described as a physical phenomenon, the parts of the equation can do well with some discussion.

### 2.2 Measuring Pedestrian Density

In physics, mass density  $\rho$  has units  $[\rho] = \frac{\text{mass}}{\text{volume}}$ . However, this does not seem to be the best fit for the problem considered here. The definition  $[\rho] = \frac{\text{mass}}{\text{area}}$  used, for example, in [?] similarly includes “mass” which the authors need to model inertial effects, which are not included in our model.

Concerning pedestrian inertial mass, we require the following assumption:

Due to the smoothness of the controlling fields we assume that it is not necessary to describe mass (inducing inertial behavior in the model). This way we assume that the pedestrians may follow (adapt speed and heading) to the controlling fields without significant lag by means of internal impetus, decision and physical strength.

Therefore, one natural way to measure the pedestrian density in this setting is to use  $[\rho] = \frac{\text{pedestrians}}{\text{area}}$ , which implicitly relies on a certain amount of homogeneity of the pedestrian crowd in the considered sample. An even smarter approach is presented in [?] by defining the area that a specific pedestrian occupies. This area depends on, e.g., whether the pedestrian is a child, an adolescent or an adult, which cloths the pedestrian wears (summer or winter cloths), how much luggage the pedestrian carries and so on. This yields an appropriate dimensionless measure  $[\rho] = \frac{\text{pedestrians' needed area}}{\text{available area}}$ . Since the area occupied by a pedestrian is not always readily available for input, we choose the former definition of density as pedestrians per area.

In our model we use normalized densities:  $\rho_i, \rho \in [0, 1]$  with  $\rho = \sum_{i=1}^n \rho_i$ . A value of  $\rho = 1$  would for instance mean  $5.4 \frac{\text{pedestrians}}{\text{area}}$  according to [?] and up to  $10 \frac{\text{pedestrians}}{\text{area}}$  according to other sources (see, e.g., [?] for a discussion).

### 2.3 Transport Velocity

The primary goal is to find a sensible functional relationship  $v_i = v_i(\rho_1, \dots, \rho_n)$  that yields a nonlinear system for realistic cases.

In the literature, one frequently discriminates between a planned (e.g., “external” in [?] or “tactical” in [?]) and an instantaneous (e.g., “intelligent” in [?] or “operational” in [?]) velocity. In our opinion, this differentiation makes sense in the context of categorizing the cause of an action taken by a pedestrian.

Our approach is slightly more pragmatic and accounts for three different types of decisions. Pedestrians:

1. choose a direction they wish to go,
2. choose a speed for walking in the chosen direction based on local conditions,
3. alter speed and walking direction in order to locally avoid densely populated areas (prefer the direction of  $-\nabla\rho$ ).

Therefore, we decompose the velocity as follows:

$$v_i = a_i V d_i^i - b_i W d^l, \quad (2)$$

where:

$V \in [0, 1]$  is a normalized speed determined by a fundamental diagram (see below).

$d_i^i$  is a unit vector field pointing into the direction of the desired heading.

$d^l$  is a directional vector field for local correction (not necessarily of unit length, see below). Since it depends on the total density  $\rho$ , it is common to all pedestrian species.

$a_i$  and  $b_i$  are constants:  $a_i$  stands for the absolute value of the wished velocity,  $b_i$  is a measure for avoiding regions of high density.

$W = 1 - V$  reflects the operational shift from wanting to reach the desired target to reacting to local encounters with other pedestrians at high densities.

Summarizing this the term  $a_i V d_i^l$  stands for the gradient driven part of the velocity and  $b_i W d^l$  decies the influence of high density regions on the velocity of pedestrians.

A model for two pedestrian species with just the  $a_i V d_i^l$  term present has been investigated in [?] with a focus on discussing the mathematical foundation. This investigation highlights some shortcomings of the model with respect to the simulation of real-world scenarios. The authors suggest to introduce (cross) diffusion terms in order to solve these problems. Since the meaning of these terms in the context of real-life applications seems to be obscure, here we prefer to introduce the  $b_i W d^l$  term.

## 2.4 Desired Heading.

The term  $d_i^l$  describes the pedestrian's choice of a walking direction, and is based on spatial information from the vicinity and the global environment of the pedestrian:

$$\Delta \phi_j^{(i)}(\vartheta) = r_j^{(i)}(\vartheta), \quad (3)$$

$$\phi_i(\vartheta) = \sum_j \phi_j^{(i)}(\vartheta), \quad (4)$$

$$d_i^l(\vartheta) = \begin{cases} \frac{\nabla \phi_i(\vartheta)}{|\nabla \phi_i(\vartheta)|} & \text{if } |\nabla \phi_i(\vartheta)| \neq 0, \\ \text{random unit vector} & \text{if } |\nabla \phi_i(\vartheta)| = 0. \end{cases}$$

With the formula (??) we add the different potentials coming from global influences like the shape of the considered domain or local influences like the local density.

The subscripted character  $j$  of  $\phi_j^{(i)}(\vartheta)$  denotes the influence type (for example global, local etc.), and the superscripted character  $i$  denotes the considered species.

Therefore, according to the assumption of continuous influences,  $d_i^l$  is based on source and boundary terms of  $j$  (partially) solved Poisson equations for each pedestrian species  $i$  (reflecting  $j$  different influencing factors). The  $\alpha_j^{(i)}$  are constant weights, and the  $f_j^{(i)}(\vartheta)$  are source terms derived from spatially distributed information—for example, the density  $\rho_k(\vartheta)$  of some pedestrian species. This kind of flow, the direction of which is derived from a potential, has been investigated in [?].

The parameters in the above equations have to be chosen very specifically, and finding appropriate settings is one of the open tasks for the application of this model.

With a special choice of the right hand side of the equation (??) we can model global or local influences by potentials. A detailed discussion of this point is given in [?].

## 2.5 Introducing the Gradient Term.

There are a number of possible approaches to introduce a gradient term. Notable are the following two:

$$d^l(\vartheta, x) = \begin{cases} \frac{\nabla\rho(\vartheta, x)}{|\nabla\rho(\vartheta, x)|} & \text{if } |\nabla\rho(\vartheta, x)| > 0, \\ 0 & \text{if } |\nabla\rho(\vartheta, x)| = 0, \end{cases} \quad (5)$$

$$d^l(\vartheta, x) = \begin{cases} \frac{\nabla\rho(\vartheta, x)}{|\nabla\rho(\vartheta, x)|} & \text{if } |\nabla\rho(\vartheta, x)| > 1, \\ \nabla\rho(\vartheta, x) & \text{else.} \end{cases} \quad (6)$$

Concerning (??) it has to be noted that  $d^l(\vartheta, x)$  is not necessarily continuous with respect to  $x$  at points where  $|\nabla\rho(\vartheta, x)| = 0$  holds. Another problem obviously present with this term is that it may show large scatter where the density is high. This can lead to the violation of the condition  $\rho_i, \rho \in [0, 1]$  because of numerical overshooting. Another risk is the numerical oscillation of the solution (which might be interpreted as remaining erratic pedestrian activity at high densities in certain situations).

This term might be viewed as carrying some random disturbances as discussed in [?,?], which produces less effective motion (stronger clogging tendency due to the “freezing by heating effect” discussed there). The measurement of the mobility there did not show an increase of flux with more “thermal” motion at all. This is due to the inhibition of lane formation because the effect of lane formation yields an enhancement of flux. The observed “freezing by heating effect” has been considered for modeling panic situations, where it might well make sense. However, such scenarios are beyond the scope of this paper.

The gradient term defined by (??) is more likely to be the rule applied by pedestrians under normal conditions, because it is more efficient than the term given by Eq. (??).

Another argument in favor for (??) is given by the fact that the key idea of the macroscopic approach is to average the behavior of several pedestrians and thus smoothing out random disturbances caused by single pedestrians at sufficiently large scales.

## 2.6 Walking Speed and Fundamental Diagram.

A uni-directional flux can be defined by  $J = \rho_i V(\rho_1, \dots, \rho_n) d_i$ . For the case of  $J = \rho V(\rho) d$  the three quantities are related by a fundamental diagram. Fundamental diagrams have been determined by a number of authors, with a relatively

wide range of different results that cannot be used to deduce a general law. According to [?], the values found in the literature for the maximum pedestrian density, where movement is possible at all, vary from  $3.8/m^2 - 10/m^2$ . Another controversially discussed issue is how  $V$  depends on whether movement is uni-directional or multi-directional.

For more details, see [?] and [?].

Despite the issues described above, we have evaluated the impact of different fundamental diagrams on quantitative and qualitative properties of the solutions. The differences are large enough to indicate the need for a better approximation in this respect. The fundamental diagrams that we have tested are:

$$\begin{aligned} V(\rho) &= 1 - \rho, \quad V(\rho) = (1 - \rho)^2, \quad V(\rho) = 1 - \rho^2, \\ V(\rho) &= 1 - \exp(-1.913/5.4(1/\rho - 1)). \end{aligned} \quad (7)$$

Note that, compared to [?, p. 65], Eq. (??) employs the normalization conditions  $V \in [0, 1]$  and  $\rho \in [0, 1]$ .

## 2.7 Simulation example - 90° Encounter.

The above discussed boundary value problem completed by appropriate boundary conditions (see [?]) is solved using the Finite-Volume package OpenFOAM. In The figures ?? show the results of two pedestrian streams crossing with an angle of 90°. A formation of dynamically reconfiguring clusters can be observed.

**Fig. 1.** Time steps 5, 10, 20, 40, 60 and 80 of the simulation of a 90° encounter of two species. Shown are density and flux of one species coming from left. The length of the arrows indicate flux strength, the grade of darkness indicates the density of the species. The crossing species coming from bottom is located in the light gray or white regions of the area

## 3 A Multispecies Pedestrian Model based on a 3d multiphase incompressible fluid flow model

The idea to simulate pedestrian flow by the application of fluid dynamics equations has a certain history in that field. This approach is based on the application of partial differential equations, which makes it a macroscopic method. The need to simulate several different species of pedestrians is a need from the start, which has not been matched very well by numerical simulations of the macroscopic type. The basis of the description of non dense pedestrian movement by incompressible fluid flow models consists in the introduction of an empty phase as a species of a multiphase system of distinct phases. In the following we describe

the mathematical model and modifications to the multiphaseInterFoam-solver of the OpenFOAM library, which makes it applicable in this field and present results that show capabilities and limitations of the modified solver.

We introduces now a new technique for the simulation of several species in macroscopic simulation of pedestrian crowds. The focus is on the modelling of several species with different destination and the ability to intersect each other rather than on a precise reconstruction of known pedestrian phenomena for prediction purposes. We proceed by first presenting the mathematical model followed by a concrete implementation and some results. Based on the discussions in [?], [?] and [?] we choose the incompressible Navier-Stokes equations as a starting point of our model and added boundary conditions and transport equations to allow an intermixing and separation of different species.

### 3.1 The Mathematical Model

We use the non-stationary, incompressible Navier-Stokes equations

$$\rho \frac{\partial \mathbf{v}}{\partial t} + \rho \mathbf{v} \cdot \nabla \otimes \mathbf{v} + \nabla p - \quad (8)$$

$$\nabla \cdot (\mu(\nabla \otimes \mathbf{v}) + \mu(\nabla \otimes \mathbf{v})^T) = \mathbf{f} \quad (9)$$

$$\nabla \cdot \mathbf{v} = \mathbf{0} \quad (10)$$

combined with a volume of fluid (VOF) method as a starting point to simulate  $N_p \in \mathbb{N}$  different pedestrian species. Let  $\mathbb{P} = \{1, \dots, N_p\}$  be the set of indices of pedestrian groups, then the VOF method keeps track of the species' positions by introducing one fraction function per species

$$\alpha_i(\mathbf{x}) \in [0, 1], \quad (11)$$

that describes the fill level at position  $\mathbf{x} \in \Omega$  of species  $i \in \mathbb{P}$ . The fraction function can be discontinuous, especially when discretized for implementation purposes. We demand the sum of all fraction functions to be one, i.e.

$$\sum_{i \in \mathbb{P}} \alpha_i = 1. \quad (12)$$

A standard VOF method uses the velocity computed by (??) with  $\rho = \sum_{i \in \mathbb{P}} \rho_i \alpha_i$ ,  $\mu = \sum_{i \in \mathbb{P}} \mu_i \alpha_i$  and changes every  $\alpha_i$  by solving the transport equation

$$\frac{\partial \alpha_i}{\partial t} + \mathbf{v} \cdot \nabla \alpha_i = 0 \text{ for all } i \in \mathbb{P}. \quad (13)$$

In the course of pedestrian simulation we tried to simulate group crossing. Therefore, it was necessary to solve three modelling problems:

1. simulation of spaces without a pedestrian species
2. distinct species forces
3. separation of species

### 3.2 Empty Spaces

An empty space is simulated by using a pedestrian group  $f \in \mathbb{P}$ ,  $\mathbb{P}_{wf} = \mathbb{P} \setminus \{f\}$ . This so-called fill-species is able to leave  $\Omega$  by flowing through an additional dimension, i.e. for a two-dimensional  $\Omega$  the third dimension or z-axis. It is therefore necessary to simulate a three dimensional domain for a two dimensional problem. The inflow and outflow over the third dimension is implemented using special boundary conditions that are aware of the fill-species. We used a solver that is based on an operator splitting approach. Therefore, we have to choose two boundary conditions; one for the velocity and one for the pressure variable. The boundary condition for the velocity is defined as

$$\mathbf{n} \cdot \mathbf{v} = 0, \text{ for } \mathbf{n} \cdot \Phi \geq 0, \alpha_f = 0 \quad (14)$$

$$\mathbf{n} \cdot \nabla(\mathbf{n} \cdot \mathbf{v}) = 0 \text{ otherwise,} \quad (15)$$

where  $\Phi$  is the velocity value adjacent to the boundary condition face from the last pressure correction step.

The pressure boundary condition is defined as

$$p = \begin{cases} p_0 - \frac{1}{2}\rho\|\mathbf{v}\|^2, & \text{for } \mathbf{n} \cdot \Phi < 0 \\ p_0, & \text{for } \mathbf{n} \cdot \Phi \geq 0, \alpha_f > 0 \end{cases} \quad (16)$$

$$\mathbf{n} \cdot \nabla p = 0, \text{ for } \mathbf{n} \cdot \Phi \geq 0, \alpha_f = 0 \quad (17)$$

$$(18)$$

on the z-axis. The other sides of the domain can be chosen as slip boundary conditions.

### 3.3 Species Forces

Each species of the intersection of pedestrians needs to have a distinct destination. Therefore the need to implement species specific forces and velocities arises. Each pedestrian species  $i \in \mathbb{P}_{wf}$  has a desired velocity  $\mathbf{v}_i^d$ , that is the velocity a pedestrian species has without the influences of other pedestrian species.

The desired velocity gets transformed into a resulting force for the right hand side in the Navier-Stokes equation (??). Following the nomenclature by Helbing et al. for microscopic models (cf. [?], [?]), we introduce a so-called behavioural force

$$\mathbf{f} := C_2(\alpha^{bil}) \left( C_1(\alpha^{bil}) \sum_{i \in \mathbb{P}_{wf}} \alpha_i \mathbf{v}_i^d - \mathbf{v} \right), \quad (19)$$

with

$$\alpha^{bil} := \sum_{i \in \mathbb{P}_{wf}} \alpha_i \quad (20)$$

and add it to the right hand side of the Navier-Stokes equations (??). The functions  $C_1$  and  $C_2$  control the pedestrian behaviour, e.g. a choice of

$$C_1(\alpha^{bil}) := (1 - \alpha^{bil}) \quad (21)$$

$$C_2(\alpha^{bil}) := \alpha^{bil} \quad (22)$$

approximates the pedestrian fundamental diagram.

### 3.4 Separation of Species

The separation of species is not naturally given by the discretized VOF method. Equation (??) does not provide a mean of separation of once mixed cells due to the fact we compute until now only a global velocity  $\mathbf{v}$  out of the Navier-Stokes equations (??). Thus, we introduce an additional transport equation

$$\frac{\partial \alpha_i}{\partial t} - \nabla \cdot \left( C_3(\alpha_f) \frac{\mathbf{v}_i^d}{\|\mathbf{v}_i^d\|} \alpha_i \right) = 0 \quad (23)$$

for all  $i \in \mathbb{P}_{\text{wb}}$  followed by

$$\alpha_f = 1 - \sum_{i \in \mathbb{P}_{\text{wf}}} \alpha_i \quad (24)$$

with  $C_3$  defining the magnitude of the separation velocity with a typical value of

$$C_3(\alpha_f) = \begin{cases} 0.01, & \text{for } \alpha_f > 0 \\ 0, & \text{for } \alpha_f = 0. \end{cases} \quad (25)$$

### 3.5 Implementation

The Navier-Stokes equation is solved using the so-called Pressure Implicit with Splitting Operators (PISO) algorithm [?] (use of the multiphaseInterFoam solver in OpenFOAM [?]). The solver consists mainly of three distinct steps. The velocity predictor step, the pressure correction loop and the fraction function adjustments. It further implements a surface tension force, which has been disabled for our experiments, but might be used in combination with our model, too.

We need to introduce some notation to proceed. We will call  $\mathcal{E}$  the set of all velocity nodes and  $\mathcal{N}(i), i \in \mathcal{E}$  the set of all neighbor nodes of  $i$ , that is the nodes whose cell share a face with the cell of  $i$ . Let us denote by  $V_i$  the volume of a cell for node  $i \in \mathcal{E}$ .

### 3.6 The velocity predictor step

Let  $\rho_g$  and  $\mu_g$  be defined as

$$\rho_g = \sum_{i \in \mathbb{P}} \rho_i \alpha_i, \quad \mu_g = \sum_{i \in \mathbb{P}} \mu_i \alpha_i, \quad (26)$$

where  $\mu_i$  and  $\rho_i$  are species dependent and  $\mathbf{f}$  be computed by (??). For the most simple case we use the explicit Euler method, so equation (??) becomes

$$\int_{V_i} \rho_g \frac{\mathbf{v}^{n+1} - \mathbf{v}^n}{\Delta t} d\mathbf{x} + \int_{\partial V_i} (\mathbf{n} \cdot \rho_g \Phi^n) \mathbf{v}^n d\mathbf{s} + \quad (27)$$

$$\int_{V_i} \nabla p^n d\mathbf{x} - \int_{V_i} \nabla \cdot (\mu_g (\nabla \otimes \mathbf{v}^n) + \mu_g (\nabla \otimes \mathbf{v}^n)^T) d\mathbf{x} \quad (28)$$

$$= \int_{V_i} \mathbf{f}^n d\mathbf{x} \quad (29)$$

in a finite volume context, where  $\Phi$  is the velocity interpolated to the faces using the values from neighbor cells and  $n$  symbolizes the current time step. OpenFOAM is using a kind of Rhie-Chow interpolation for flux fields, which we will symbolize by  $\Pi$ .

Then the algebraic equation for a single cell  $i \in \mathcal{E}$  of (??) becomes

$$a_i \mathbf{v}_i + \sum_{n \in \mathcal{N}(i)} a_n \mathbf{v}_n = \mathbf{b}_i - \nabla p_i \quad (30)$$

in discretized form, where  $a_i \in \mathbb{R}$  are the coefficients for  $\mathbf{v}_i$  and  $\mathbf{b}$  represents the right hand side of the algebraic equation without the pressure.

### 3.7 The pressure correction loop

Let  $A$  be the diagonal matrix containing all  $a_i$  from equation (??), that is for  $k = \lfloor j/3 \rfloor$  let  $(A)_{jj} = a_k$  and  $(A)_{ij} = 0$  for  $i \neq j$  and further let  $H$  be the vector containing all  $a_n \mathbf{v}_n$  and the right hand side  $\mathbf{b}_i$ , that is

$$H_{3i+j} = (- \sum_{n \in \mathcal{N}(i)} a_n \mathbf{v}_n + \mathbf{b}_i)_j \text{ for } j \in \{1, 2, 3\}. \quad (31)$$

This H-operator is common for OpenFOAM based implementations. We then compute a Jacobi step for  $\mathbf{v}$  with

$$\mathbf{v}_{\text{jac}} = A^{-1} H \quad (32)$$

Next, we compute  $\Phi = \Pi(\mathbf{v}_{\text{jac}} + A^{-1} \mathbf{f})$  followed by

$$\nabla \cdot (A^{-1} \nabla p^{n+1}) = \nabla \cdot \Phi \quad (33)$$

to compute the new  $p^{n+1}$ .

The face flux  $\Phi$  is then corrected by

$$\Phi^{n+1} = \Pi(A^{-1} H - A^{-1} \nabla p) \quad (34)$$

followed by the correction of the velocity

$$\mathbf{v}^{n+1} = \mathbf{v}_{\text{jac}} - \nabla p. \quad (35)$$

The boundary conditions (??) and (??) are used for the z-axis in equations (??) and (??), respectively. The velocity's boundary conditions have been set to slip at non-penetrable walls and boundary conditions for the pressure have been chosen as zero gradient. The pressure correction loop is repeated until the pressure converges or a maximum number of rounds is reached.

### 3.8 Adjustment of the Fraction Function

The computation of  $\mathbf{v}^{n+1}$  allows the adjustment of the fraction function via (??). It follows the separation of the species by solving (??) and (??). Usually a downwind scheme should be used for the evaluation of  $C_3$ , so it is set depending on the  $\alpha_f$  value in the target cell.

When the fraction function has been adjusted, the velocity predictor step continues with the next time step.

### 3.9 Numerical Results

We produced simulation results for quadratic geometries with an orthogonal mesh and on a more complex geometry inspired by real world experiments in the Technical University of Berlin [?].

Fig. ?? shows the results for a quadratic area with two species crossing in 180 degrees.

As can be seen from Fig. ?? the species cross each other, show stripe formation, create lanes and reach their destination on opposite walls. At the end of the simulation the species are completely separated. It should, however, be noted, there are several effects originating in the impulse conservation, which are rather unnatural for crowd simulation. For example the occurrence of a splash at the moment the species hit a wall with larger values of  $\mathbf{v}$ , which is due to the impulse conservation and can be seen at time  $T = 20.0$  in Fig. ?. There, one is able to see species one splashing back at the bottom wall. Further, the masses have a non-neglectable acceleration time, which is in contrast to pedestrians behaviour.

We made real world experiments, that can be used to test parameters and validate the numerical results. In 2010 and 2011 we performed several experiments with up to four crowd groups that were crossing in a predefined area. The experiments have been recorded on video and we were able to observe common crowd phenomena like lane formation and isolated groups (c.f. [?]). It also allowed us to get quantitative results for evaluation purposes by video analysis [?].

Therefore, we made numerical simulation on a mesh with a geometry similar to the control area in the real world experiments. The simulation in the control area shows lane formation and congestion before an entrance, see Fig. ?. The origin of the congestion lays in the very static desired velocities we are currently using. A more dynamical desired velocity that better models pedestrian long and short sight behaviour is subject of future work.

Experiments showed the fill-species and the pedestrian species should have the same density  $\rho$ . Otherwise, we may create artificial impulses through the separation step that could move heavier species to a place with higher velocity. Although different  $\rho$  values for different species will work, the impulse balance should be kept in mind.

We were also able to implement very basic in- and outlet boundary conditions for multiple species, i.e. the fill-species and a pedestrian species. For inlet boundaries we use a fixed value condition for the velocity together with the pressure boundary condition (??). For outlet boundary conditions we use (??) and (??) for the pressure and velocity, respectively. Further research should be put in in- and outlet boundary conditions for more complex in- and outflow scenarios of pedestrian, e.g. the rate of flow should be controllable depending on the fill rate of cells next to the inlet boundary.

## 4 Discussion

In section ?? we presented a macroscopic model based on the mass balance with velocity ansatzes respecting local and global influences. The numerical simulation results of the densities and the fluxes (pedestrian velocities) matched the experimental data with a good quality. Especially typical patterns of crossing pedestrian groups and time scales of processes like emptying were very good reproduced. The simulation results are promising and in our further research we have to investigate the detailed description of model parameters with the aim of a reduction of the occurring heuristic parameters. For special constellations like the genesis of small groups moving close together the fundamental diagrams must be appropriately modified.

In section ?? we introduced a new ansatz for the simulation of pedestrian crossing and multispecies simulation. The implementation is based on the incompressible Navier-Stokes equations with a volume of fluid ansatz that has been altered by special boundary conditions for the pressure and the velocity as well as an added transport equation for the separation of intermixed species. The proposed model allowed us to reproduce common pedestrian crossing effects like stripe and lane formation. It also allows us to simulate higher numbers (more than two) of pedestrian species.

The model showed impulse effects originating from the Navier-Stokes equations, which are unnatural for pedestrian behaviour. Therefore, it is the subject of future work to use a different set of equations and to study the stability and conservation properties of the solver in more detail. Another topic is the implementation of open boundaries for the in- and outflow of pedestrians in the simulation.

## References

1. Chen, M.J., Bärwolff, G., Schwandt, H.: A study of step calculations in traffic cellular automaton models. In: 13th International IEEE Conference on Intelli-

- gent Transportation Systems. (2010) 747–752 An electronic version can be retrieved at: <http://page.math.tu-berlin.de/~chenmin/pub/cbs100709.pdf> (accessed July 12, 2013).
2. Lämmel, G., Plaue, M.: Getting out of the way: collision avoiding pedestrian models. PED 2012 Conference Proceedings (2012)
  3. Moussaïd, M., Helbing, D., Theraulaz, G.: How simple rules determine pedestrian behavior and crowd disasters. PNAS **108**(17) (April 2011) 6884–6888
  4. Predtechenskii, V.M., Milinskii, A.I.: Planning for Foot Traffic Flow in Buildings. Amerind Publishing, New Delhi (1978) translation of Proekttirovanie Zhdanii s. Uchetom Organizatsii Dvizheniya Lyuddskikh Potokov (Moscow: Stroiizdat, 1969).
  5. Weidmann, U.: Transporttechnik der Fußgänger – transporttechnische Eigenschaften des Fußgängerverkehrs (Literaturstudie). Schriftenreihe der IVT **90** (March 1993) in German.
  6. Schadschneider, A., Klingsch, W., Kluepfel, H., Kretz, T., Rogsch, C., Seyfried, A.: Evacuation dynamics: Empirical results, modeling and applications. Encyclopedia of Complexity and Systems Science (2009) 3142–3176
  7. Cristiani, E., Piccoli, B., Tosin, A.: Modeling self-organization in pedestrians and animal groups from macroscopic and microscopic viewpoints. In Bellomo, N., Naldi, G., Pareschi, L., Toscani, G., eds.: Mathematical Modeling of Collective Behavior in Socio-Economic and Life Sciences. Modeling and Simulation in Science, Engineering and Technology. Birkhäuser Boston (2010) 337–364
  8. Berres, S., Ruiz-Baier, R., Schwandt, H., Tory, E.M.: An adaptive finite-volume method for a model of two-phase pedestrian flow. Networks and Heterogeneous Media (NHM) **6** (2011)
  9. Hughes, R.L.: A continuum theory for the flow of pedestrians. Transportation Research Part B **36** (2002) 507–535
  10. Huth, F., Bärwolff, G., Schwandt, H.: A macroscopic multiple species pedestrian flow model based on heuristics implemented with finite volumes. PED 2012 Conference Proceedings (2012)
  11. Helbing, D., Farkas, I.J., Vicsek, T.: Freezing by heating in a driven mesoscopic system. Phys. Rev. Lett. **84**(6) (Feb 2000) 1240–1243
  12. Radzihovsky, L., Clark, N.A.: Comment on “Freezing by heating in a driven mesoscopic system”. Phys. Rev. Lett. **90**(18) (May 2003) 189603
  13. Huth, F., Bärwolff, G., Schwandt, H.: Some fundamental considerations for the application of macroscopic models in the field of pedestrian crowd simulation. Preprint ID 2012/16 at [http://www.math.tu-berlin.de/menue/forschung/veroeffentlichungen/preprints\\_2012](http://www.math.tu-berlin.de/menue/forschung/veroeffentlichungen/preprints_2012) (2012)
  14. Huth, F., Bärwolff, G., Schwandt, H.: Fundamental diagrams and multiple pedestrian streams. Preprint ID 2012/17 at [http://www.math.tu-berlin.de/menue/forschung/veroeffentlichungen/preprints\\_2012/](http://www.math.tu-berlin.de/menue/forschung/veroeffentlichungen/preprints_2012/) (2012)
  15. Bärwolff, G., Slawig, T., Schwandt, H.: Modeling of pedestrian flows using hybrid models of euler equations and dynamical systems. AIP Conference Proceedings **936**(1) (2007) 70–73
  16. Henderson, L.F.: The Statistics of Crowd Fluids. Nature **229**(5284) (February 1971) 381–383
  17. Ahnert, T., Bärwolff, G., Schwandt, H.: A Multispecies Macroscopic Pedestrian Model approximated by a 3d incompressible Flow. Proceedings of the 7th International Conference on Information and Management Sciences 2012 in Dunhuang/China (California Polytechnic State University Press, Series of Information and Management Sciences, Vol. 7, Pomona, California) (2012) 475-480

18. Helbing, D., Molnár, P.: Social force model for pedestrian dynamics. *Phys. Rev. E* **51** (May 1995) 4282–4286
19. Johansson, A., Helbing, D., Shukla, P.: Specification of the social force pedestrian model by evolutionary adjustment to video tracking data. *Advances in Complex Systems* (10) (2007) 271–288
20. Issa, R.I.: Solution of the implicitly discretised fluid flow equations by operator-splitting. *Journal of Computational Physics* (62) (1986)
21. Ltd., O.: OpenFOAM: The open source CFD toolbox (2010) Webpage: <http://www.openfoam.com> (accessed July 12, 2013).
22. Plaue, M., Chen, M., Bärwolff, G., Schwandt, H.: Trajectory extraction and density analysis of intersecting pedestrian flows from video recordings. In Stilla, U., Rottensteiner, F., Mayer, H., Jutzi, B., Butenuth, M., eds.: *Photogrammetric Image Analysis*. Volume 6952 of *Lecture Notes in Computer Science*. Springer Berlin / Heidelberg (2011) 285–296 10.1007/978-3-642-24393-6\_24.

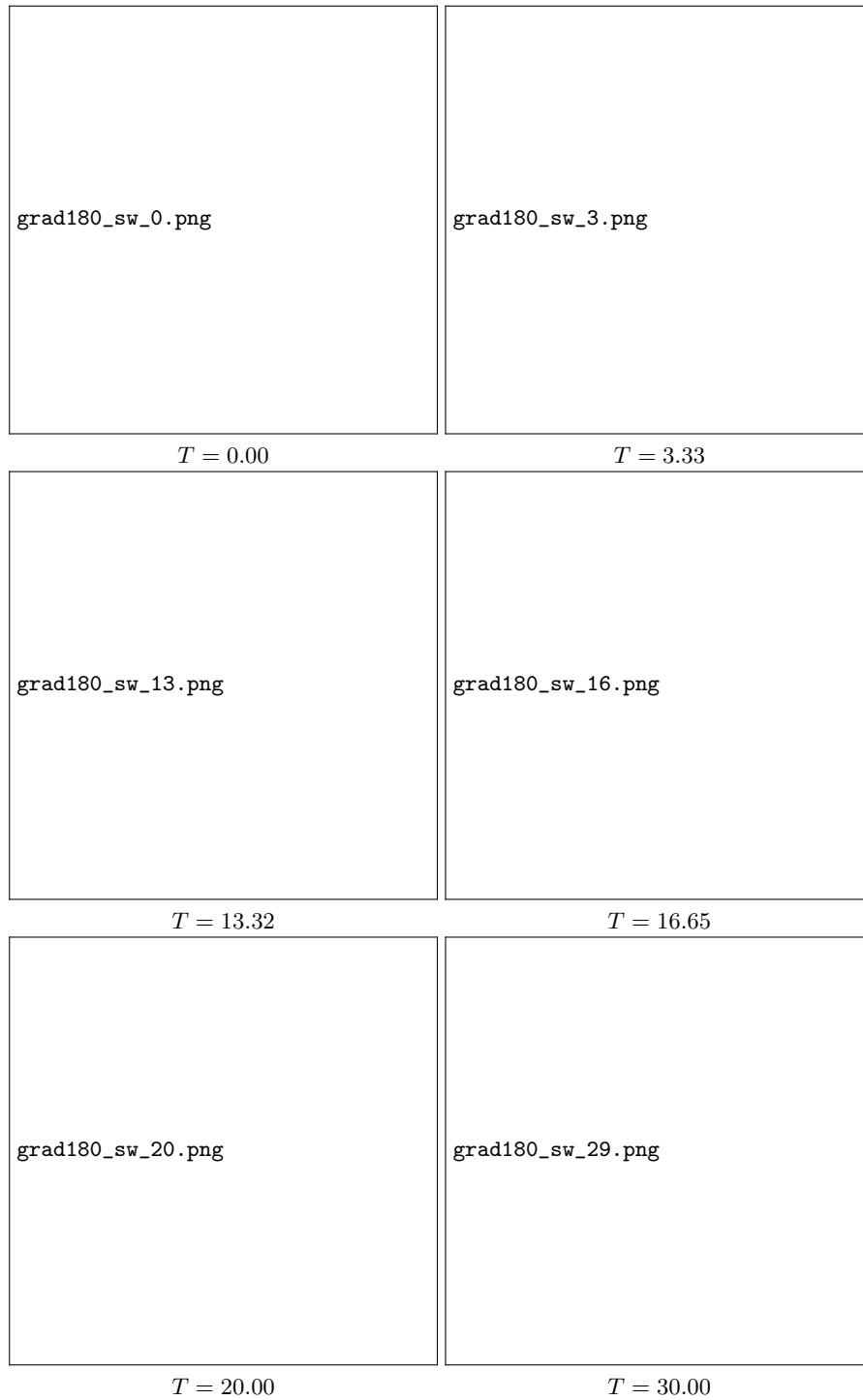


**Fig. 2.** Simulation of  $180^\circ$  crossing with  $\max(\mathbf{u}) = 10.0$ ,  $\mathbf{v}_{ps} = 0.04$ ,  $\max(|\mathbf{f}|) = 1000$  as parameters.

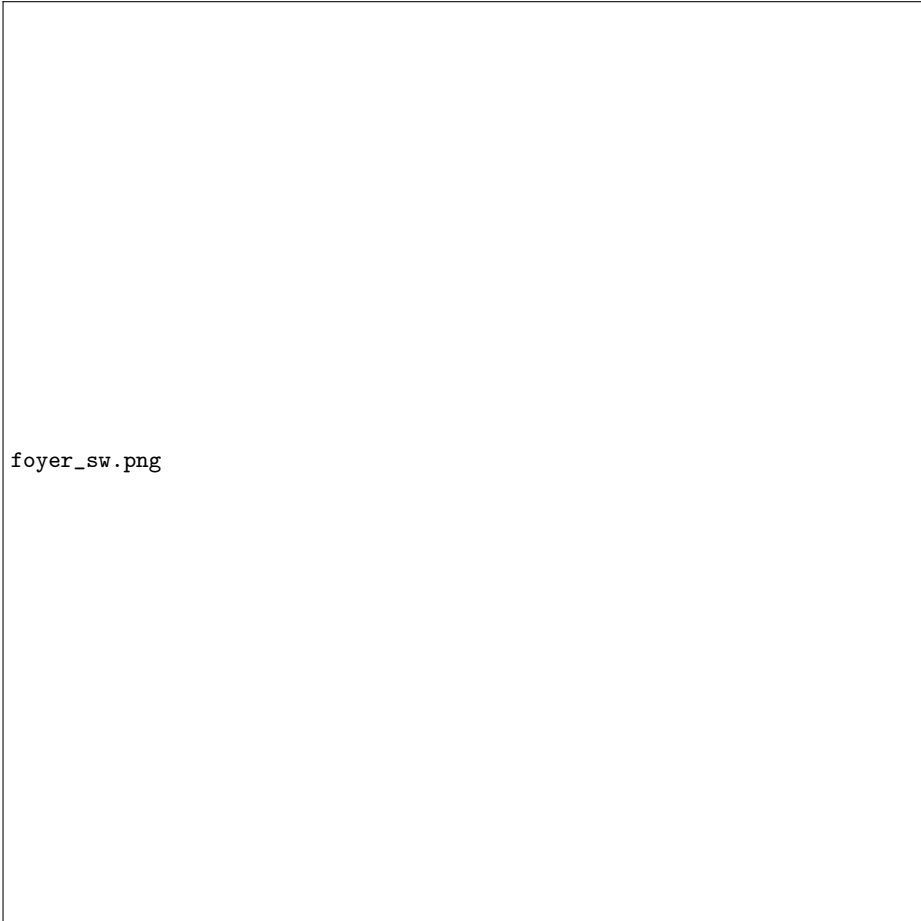


**Fig. 3.** Simulation done with a complex geometry inspired by real world experiments.